

Lower clearance of sodium tanshinone IIA sulfonate in coronary heart disease patients and the effect of total bilirubin: a population pharmacokinetics analysis

QIN Wei-Wei^{1Δ}, WANG Li^{1Δ}, JIAO Zheng^{1*}, WANG Bin^{1*}, WANG Cheng-Yu¹,
QIAN Li-Xuan¹, QI Wei-Lin², ZHONG Ming-Kang¹

¹ Department of Pharmacy, Huashan Hospital, Fudan University, Shanghai, 200040, China;

² Department of Cardiology, Huashan Hospital, Fudan University, Shanghai, 200040, China

Available online 20 Mar., 2019

[ABSTRACT] This study developed a population pharmacokinetic model for sodium tanshinone IIA sulfonate (STS) in healthy volunteers and coronary heart disease (CHD) patients in order to identify significant covariates for the pharmacokinetics of STS. Blood samples were obtained by intense sampling approach from 10 healthy volunteers and sparse sampling from 25 CHD patients, and a population pharmacokinetic analysis was performed by nonlinear mixed-effect modeling. The final model was evaluated by bootstrap and visual predictive check. A total of 230 plasma concentrations were included, 137 from healthy volunteers and 93 from CHD patients. It was a two-compartment model with first-order elimination. The typical value of the apparent clearance (CL) of STS in CHD patients with total bilirubin (TBIL) level of $10 \mu\text{mol}\cdot\text{L}^{-1}$ was $48.7 \text{ L}\cdot\text{h}^{-1}$ with inter individual variability of 27.4%, whereas that in healthy volunteers with the same TBIL level was $63.1 \text{ L}\cdot\text{h}^{-1}$. Residual variability was described by a proportional error model and estimated at 5.2%. The CL of STS in CHD patients was lower than that in healthy volunteers and decreased when TBIL levels increased. The bootstrap and visual predictive check confirmed the stability and validity of the final model. These results suggested that STS dosage adjustment might be considered based on TBIL levels in CHD patients.

[KEY WORDS] Sodium tanshinone IIA sulfonate; Nonlinear mixed-effects modeling; Population pharmacokinetics; Coronary heart disease; Total bilirubin

[CLC Number] R969.1 **[Document code]** A **[Article ID]** 2095-6975(2019)03-0218-09

Introduction

Sodium tanshinone IIA sulfonate (STS) is a derivative of tanshinone IIA (TSA), which is the most effective extract isolated from the root of *Salvia miltiorrhiza* (Danshen) [1-2]. Danshen is a well-known traditional Chinese medicine used

to treat cardiovascular disease [2]. Because of its high lipophilicity, TSA is poorly absorbed and cannot be used directly in the clinic. As a result, STS was developed by sulfonation of TSA in order to improve its water solubility [1-2]. Because of the pharmacological activity of TSA, STS represents a cardioprotective substance that exhibits the therapeutic antioxidant, anti-inflammatory, antiplatelet aggregation, and vasorelaxation effects [1]. STS injection has been used to treat coronary heart disease (CHD), angina pectoris, and myocardial infarction in clinical practice for more than 30 years [3].

Following intravenous (i.v.) administration in rats, STS mainly distributes to the liver, lungs, intestines, kidneys, and heart [4-5] and inhibits the activity of cytochrome P450 (CYP) 3A4 while CYP1A2, CYP2A6, CYP2C9, CYP2D6, CYP2E1, and CYP2C19 show minimal or no effects concerning the STS metabolism *in vitro* [6]. Because TSA is metabolized predominantly by NAD(P)H: quinoneoxidoreductase 1 (NQO1), NQO1 might play an important role in STS metabo-

[Received on] 12-Oct.-2018

[Research funding] This work was supported by the Science and Technology Commission of Shanghai Municipality (12DZ1930300, 12DZ1930302, 12DZ1930303), the Weak Discipline Construction Project (No. 2016ZB0301-01), and the 2016 Key Clinical Program of Clinical Pharmacy of Shanghai Municipal Commission of Health and Family Planning.

[*Corresponding author] Tel: 86-21-52888712, E-mail: zjiao@fudan.edu.cn (JIAO Zheng); Tel: 86-21-52888379, E-mail: wangbin@huashan.org.cn (WANG Bin)

^ΔThese authors contributed to the work equally.

These authors have no conflict of interest to declare.

Published by Elsevier B.V. All rights reserved

lism [7]. STS and its metabolites are secreted in the bile [8–9]. A recent study revealing the pharmacokinetics (PK) of STS in healthy volunteers showed that STS is eliminated from the body quickly, with an average clearance of $55.6 \pm 11.0 \text{ L}\cdot\text{h}^{-1}$ [10]. However, considering a different patient population and medication regimen, the PK profile could be different when STS is administered to CHD patients. Additionally, CHD patients might suffer from acute heart failure, which could result in diminished blood flow to organs of elimination [11]. A previous study indicated that patients with heart failure displayed significantly lower clearance of lidocaine as compared with that of patients without heart failure ($P < 0.005$) [12]. Moreover, various medications are used to treat CHD, and these might interact with STS [8, 13]. However, whether the PK of STS are affected by CHD and concomitant medications in clinical practice remains unclear.

In this study, we investigated the potential effects of CHD on the PK of STS. We used population pharmacokinetics (PPK) analysis to assess patient demographics, with biochemical tests, disease-related properties, and concomitant medications as covariates. These findings provide beneficial information for the safe clinical use of STS in patients with CHD.

Materials and methods

Subjects

CHD patients from Huashan Hospital (Shanghai, China) were enrolled in this prospective and observational study during the period from September 2014 to May 2015. Data from 10 healthy volunteers from a previous STS PK study were pooled into the population analysis [10]. The protocols for the clinical pharmacokinetic study of healthy volunteers and CHD patients were approved by the Institutional Ethics Committee of Shanghai Xuhui Central Hospital and Huashan Hospital, Fudan University, respectively, and were conducted according to the recommendations described in the Declaration of Helsinki. Informed consent was obtained from all participants before enrollment.

Healthy volunteers had to be qualified during medical history reviews, physical examinations, and laboratory tests. Volunteers were excluded if they were participating in other clinical studies, reported alcohol or smoking addiction, or had taken drugs within 30 days (including common medications and abused drugs involving opium, methamphetamines, ketamine, and cocaine, etc.).

CHD patients of both sexes (> 18 years of age) with confirmed CHD and undergoing STS treatment were eligible for the study. CHD patients included those with stable angina, unstable angina, and non-ST-elevation myocardial infarction [11, 14]. Patients with cancer, abnormal renal function (serum creatinine $\geq 130 \mu\text{mol}\cdot\text{L}^{-1}$) or liver function [alanine aminotransferase (ALT) $\geq 120 \text{ U}\cdot\text{L}^{-1}$], chronic heart failure due to left ventricular dysfunction, an obvious tendency for bleeding, uncontrolled hypertension (systolic blood pressure $\geq 180 \text{ mmHg}$

or diastolic blood pressure $\geq 100 \text{ mmHg}$), a history of allergies to *Salvia miltiorrhiza*, taking other Traditional Chinese Medicines, participating in other interventional clinical studies within 1 month, or currently pregnant were excluded.

Blood sampling

All healthy volunteers and CHD patients received a single i.v. dose of 40 mg STS ($0.16 \text{ mg}\cdot\text{mL}^{-1}$) over approximately 60 min. STS injection was obtained from the First Shanghai Biochemical & Pharmaceutical Co., Ltd. (Shanghai, China).

Blood samples from the healthy volunteers were obtained before and 0.167, 0.333, 0.667, 1, 1.04, 1.08, 1.17, 1.25, 1.33, 1.67, 2, 3, 5 and 7 h after initiating the infusion. Healthy volunteers fasted overnight before administering STS.

Blood samples from CHD patients were obtained before and 1, 1.83, and 3.5 h after initiating the infusion. CHD patients were not necessarily fasted before injection of STS and were not given any other medication during infusion. To the best of our knowledge, there are no published investigations regarding food influences on STS. This is likely because STS is injected directly by i.v. and not absorbed via the gastrointestinal tract; therefore, it is not affected by food.

Obtained plasma was frozen at $-20 \text{ }^\circ\text{C}$ in coded polypropylene tubes until analysis.

Bioanalytical methods

Liquid chromatography-tandem mass spectrometry (LC-MS/MS) was used to determine STS levels in human plasma, as previously described [10]. Calibration curves for STS in human plasma were linear over a range of 2 to 1000 $\text{ng}\cdot\text{mL}^{-1}$, with a lower limit of quantification at 2 $\text{ng}\cdot\text{mL}^{-1}$. The precision [% coefficient of variation (CV)] and accuracy (% bias) of the quality control (QC) samples at five concentrations were < 8% and from -7% to 5%, respectively. All blood samples from health volunteers and CHD patients were analyzed in the same laboratory at the Central Laboratory, Shanghai Xuhui Central Hospital (Shanghai, China).

PPK model development

PPK analysis was performed using a nonlinear mixed-effects modeling approach using NONMEM (v7.3; Icon Development Solutions, Ellicott, MD, USA). Perl-speaks-NONMEM (v4.2.0), Pirana (v2.9.0), and Xpose (v4.4.1) were used for model development, visual diagnostics, and model evaluation [15–17]. A first-order conditional-estimation method with η - ϵ interaction (FOCE-I) was used for parameter estimation.

One-, two-, and three-compartment models with first-order elimination were tested to develop the structural model. PK parameters were assumed to be log-normally distributed. The inter-individual variability (IIV) for the PK parameters was evaluated using an exponential model (Equation 1).

$$\theta_i = \theta_{TV} \times e^{\eta_i} \quad (1)$$

where θ_i is the parameter estimate for individual i , θ_{TV} is the typical value for the parameter of the population, and η_i is the IIV for individual i , which follows a normal distribution with a mean of zero and a variance of ω^2 . Various residual error

models, including additive, exponential, proportional, and mixed models, were fitted to describe the residual variability (Equations 2–5).

$$Y = \text{IPRED} + \varepsilon \quad (2)$$

$$Y = \text{IPRED} \times (1 + \varepsilon) \quad (3)$$

$$Y = \text{IPRED} \times \exp(\varepsilon) \quad (4)$$

$$Y = \text{IPRED} \times \exp(\varepsilon_1) + \varepsilon_2 \quad (5)$$

Various covariates were examined, including patient demographics, biochemical tests, disease-related properties, and concomitant medications. Continuous covariates included age, weight, aspartate aminotransferase, ALT, total bilirubin (TBIL), blood urea nitrogen, serum creatinine, and endogenous creatinine-clearance rate calculated by the Cockcroft–Gault equation. Categorical covariates included gender, CHD, stable angina, unstable angina, non-ST-elevation myocardial infarction, acute heart failure, and co-therapy with antiplatelet medication, β -blockers, angiotensin converting enzyme inhibitors, angiotensin II type 1 receptor antagonists (ARBs), calcium channel blockers, and statins.

Plots of covariates against empirical Bayesian estimates of individual parameters were first used to explore the association between covariates and PK parameters. Potentially significant covariates were then screened in a stepwise manner by NONMEM. A difference in objective function value (OFV) was used to evaluate the influence. Each forward step added a covariate to the model according to the reduction in OFV until there was no further significant reduction; then, each backward step removed a covariate from the model until no significant OFV reduction was observed. The criteria of significance in the forward addition steps were set at $\Delta\text{OFV} \geq 3.84$ ($P < 0.05$; $\text{df} = 1$), and the backward elimination steps were set at $\Delta\text{OFV} \geq 6.64$ ($P < 0.01$; $\text{df} = 1$). Additional criteria for the retention of a covariate included reductions in unexplained IIV, clinical significance, and biological plausibility.

Linear (Equation 6), linear proportional (Equation 7), and power model with the covariate (Cov) normalized to the population median (Equation 8) were used to describe the relationship between continuous covariates and PK parameters. Categorical covariates were modeled as shown in Equation 9.

$$P = \theta_1 \times \left(\frac{\text{Cov}_i}{\text{Cov}_m} \right) \quad (6)$$

$$P = \theta_1 + \theta_2 \times (\text{Cov}_i - \text{Cov}_m) \quad (7)$$

$$P = \theta_1 \times \left(\frac{\text{Cov}_i}{\text{Cov}_m} \right)^{\theta_2} \quad (8)$$

$$P = \theta_1 + \theta_2 \times \text{Cov}_1 + \theta_3 \times \text{Cov}_2 + \dots + \theta_{i-1} \times \text{Cov}_i \quad (9)$$

where θ is the estimated parameter, and θ_1 represents the typical value of a PK parameter of an individual with the median value of the covariate. Cov_i represents the value of the covariate for the i^{th} subject, and Cov_m represents the median value of the covariate.

Model evaluation

The model was checked by goodness-of-fit (GOF) diagnostic plots, which included predicted versus observed con-

centration and conditional weighted residuals versus observed concentration and time.

The precision and robustness of the final model were further evaluated by non-parametric bootstrap analysis. The bootstrap datasets were re-sampled from the original dataset by replacement, and each bootstrap dataset contained the same number of patients as the original dataset. The model was fitted to 1000 re-sampling datasets to obtain bootstrap parameter estimates. The 2.5% and 97.5% of each estimated parameter derived from the bootstrap datasets were compared with the mean of the parameter estimated from the final model.

Simulation-based diagnosis was conducted by visual predictive check (VPC). The procedure obtained the concentration-time curves of the datasets simulated from the final parameters via 1000 Monte Carlo simulations, followed by comparison of the 10th, 50th, and 90th percentiles of the simulated concentration-time curves with the observed concentrations in order to demonstrate overlap and variability.

Results

Subjects

Twenty-six CHD patients were enrolled in the study, and one patient dropped out because of personal reasons. The lower limit of quantification (LOQ) was 2 ng·mL⁻¹ in the analytical method. The STS concentrations of 14 blood samples were < 2 ng·mL⁻¹ and could not be determined. Therefore, these 14 blood samples were treated as missing data, one from a CHD patient and 13 from healthy volunteers. Seven observations from seven patients were missing due to patient compliance during data collection. Samples that were lower than the LOQ or missing were excluded from the analysis. A total of 137 observations from 10 healthy volunteers and 93 observations from 25 CHD patients were pooled into the final analysis.

The demographics, laboratory tests, disease-related properties, and concomitant medication information for the CHD patients and the healthy volunteers were collected (Table 1). Medications co-administered in > 10% of the CHD patients included aspirin, clopidogrel, metoprolol, bisoprolol, benazepril, perindopril, nifedipine, amlodipine, rosuvastatin, and atorvastatin (Table 1). Due to the limited sample size, medications administered to < 10% of the CHD patients were coded as groups according to their therapeutic categories. Therefore, olmesartan, irbesartan, losartan, and valsartan were coded as ARBs.

PPK model

A two-compartment model with first elimination was chosen as the structured model (subroutine ADVAN3 and TRANS4) according to the Akaike information criterion (AIC) and diagnostic plots. Because the IIVs of the distribution volumes of the central and peripheral compartments were < 1%, they were not estimated. Only the IIV of the CL and inter-compartment clearance (Q) was included in the subsequent analysis. Moreover, a proportional error model best described the residual variability.

Table 1 Summary of subjects' characters

Parameters	CHD patients	Healthy volunteers
Demographics		
Age (years)	63 (28–80), 61.8 (14.1)	25.5 (22–34), 27.2 (4.5)
Weight (kg)	65 (43–100), 66.9 (12.9)	66.1 (56.5–75.2), 64.9 (5.5)
Gender (female/male)	12/13	0/10
Laboratory tests		
PLT ($\times 10^9$)	174 (98–356), 186 (40.5)	145 (127–292), 152 (32.3)
ALT ($U \cdot L^{-1}$)	28 (10–92), 31.2 (20.1)	12 (4–19), 11.8 (4.7)
AST ($U \cdot L^{-1}$)	19 (12–81), 24.8 (14.4)	16.5 (12–24), 16.7 (3.4)
TBIL ($\mu\text{mol} \cdot L^{-1}$)	11.0 (5.2–33.7), 10.5 (5.7)	10.2 (4.9–19.2), 10.6 (4.6)
BUN ($\text{mmol} \cdot L^{-1}$)	5.6 (2.9–9.0), 5.6(1.9)	4.3 (2.8–7.3), 4.8 (1.6)
SCr ($\mu\text{mol} \cdot L^{-1}$)	62 (45–125), 66.7 (19.2)	71.5 (64–81), 72.1 (5.3)
CLcr ($L \cdot h^{-1}$)	88 (37–173), 93.8 (33.6)	123 (108–165), 125 (16.8)
Disease related characteristics		
Stable angina (<i>n</i> , %)	9 (36)	0 (0)
Unstable angina (<i>n</i> , %)	13 (52)	0 (0)
NSTEMI (<i>n</i> , %)	3 (12)	0 (0)
Acute heart failure (<i>n</i> , %)	5 (20)	0 (0)
Co-medication		
Aspirin (<i>n</i> , %)	19 (76)	0 (0)
Clopidogrel (<i>n</i> , %)	18 (72)	0 (0)
Metoprolol (<i>n</i> , %)	12 (48)	0 (0)
Bisoprolol (<i>n</i> , %)	3 (12)	0 (0)
Rosuvastatin (<i>n</i> , %)	13 (52)	0 (0)
Atorvastatin (<i>n</i> , %)	6 (24)	0 (0)
Benazepril (<i>n</i> , %)	11 (44)	0 (0)
Perindopril (<i>n</i> , %)	5 (20)	0 (0)
Olmесartan (<i>n</i> , %)	2 (8)	0 (0)
Irbesartan (<i>n</i> , %)	1 (4)	0 (0)
Losartan (<i>n</i> , %)	1 (4)	0 (0)
Valsartan (<i>n</i> , %)	2 (8)	0 (0)
Nifedipine (<i>n</i> , %)	3 (12)	0 (0)
Amlodipine (<i>n</i> , %)	5 (20)	0 (0)

Data is presented as median (range), mean (SD). PLT: platelet count, ALT: alanine aminotransferase, AST: aspartate aminotransferase, TBIL: total bilirubin, BUN: blood urea nitrogen, SCr: serum creatinine, CLcr: endogenous creatinine clearance rate calculated by Cockcroft–Gault equation, NSTEMI: Non-ST-elevation myocardial infarction

Plots of TBIL against empirical Bayesian estimates of individual parameters showed that TBIL had an influence on the CL of STS in the CHD patients, whereas it did not show a significant association with the CL in healthy volunteers. We evaluated the effects of covariates on the PK parameters of CL and Q using stepwise covariate screening. During the forward-inclusion steps, TBIL and co-administration of ARBs or statins were identified as having an effect on CL, whereas age and non-ST-elevation myocardial infarction were identified as having an effect on Q. After the backward-elimination steps, only TBIL significantly improved the CL prediction

and was retained in the final model. Removal of TBIL resulted in a significant increase in OFV (26.52; $P < 0.001$). The linear relationship described the association between TBIL and CL better than the nonlinear model. The final CL model for STS was calculated as follows (Equation 10):

$$CL = 63.1 \times \left[1 - 0.228 \times \text{CHD} \times \left(\frac{\text{TBIL}}{10} \right) \right] \quad (10)$$

where TBIL is given as $\mu\text{mol} \cdot L^{-1}$, and CHD is 1 when the subject is a CHD patient (otherwise CHD is 0).

Compared with the base model, TBIL explained approximately 42% of the IIV of CL and 5% of the residual

variability (Table 2).

A 5000 times Monte Carlo simulation was performed to describe the relationship between TBIL and CL (Fig. 1). The simulation indicated that the CL of STS in CHD patients (Fig. 1A) differed from that in healthy volunteers (Fig. 1B) and was affected by TBIL.

Model evaluation

GOF plots demonstrated adequate predictive performance of the final model (Fig. 2). The population- and individual-

predicted concentrations versus observed concentrations showed good correlation, and the conditional weighted residuals (CWRES) distributed symmetrically between -3.5 and +3.5 units.

During the bootstrap runs, 984 bootstraps provided an acceptable estimation. The values of the parameter estimates obtained from the final model were all contained within the 2.5% to 97.5% bootstrap estimates, indicating the precision and stability of the final model (Table 2).

Table 2 Parameter estimates and bootstrap results of final model

Parameters	Final model		Bootstrap	
	Estimates	RSE (%)	median	95% CI
CL (L·h ⁻¹) (θ_{CL})	63.1	5	61.8	(56.8, 66.1)
V1 (L)	7.2	6	7.0	(6.4, 7.9)
Q (L·h ⁻¹)	3.4	10	3.6	(2.8, 4.7)
V2 (L)	5.9	13	5.8	(4.7, 6.8)
TBIL_CL(θ_{TBIL})	-0.23	5	-0.23	(-0.24, -0.082)
Inter-individual variability				
ω_{CL} (CV%)	16.6	18	16.3	(9.6, 20.5)
Ω_Q (CV%)	20.7	76	26.3	(4.6, 41.8)
Residual Error				
Proportional (%)	5.2	24	5.0	(3.5, 8.0)

CI = confidence interval; RSE = relative standard error.

The final population pharmacokinetic model is:

$$CL = \theta_{CL} \times \left[1 - \theta_{TBIL} \times CHD \times \left(\frac{TBIL}{10} \right) \right], \text{ CHD is 1 when the subject is a CHD patient, otherwise CHD is 0.}$$

CL = apparent clearance; V1 = the apparent volume of the central compartment; Q = inter compartment clearance; V2 = the apparent volume of the peripheral compartment; TBIL_CL = the influence of total bilirubin on CL; C = coefficient of variation. Percentile bootstrap 95%CI corresponding to parameter estimates at the 2.5th and 97.5th percentiles of bootstrap runs

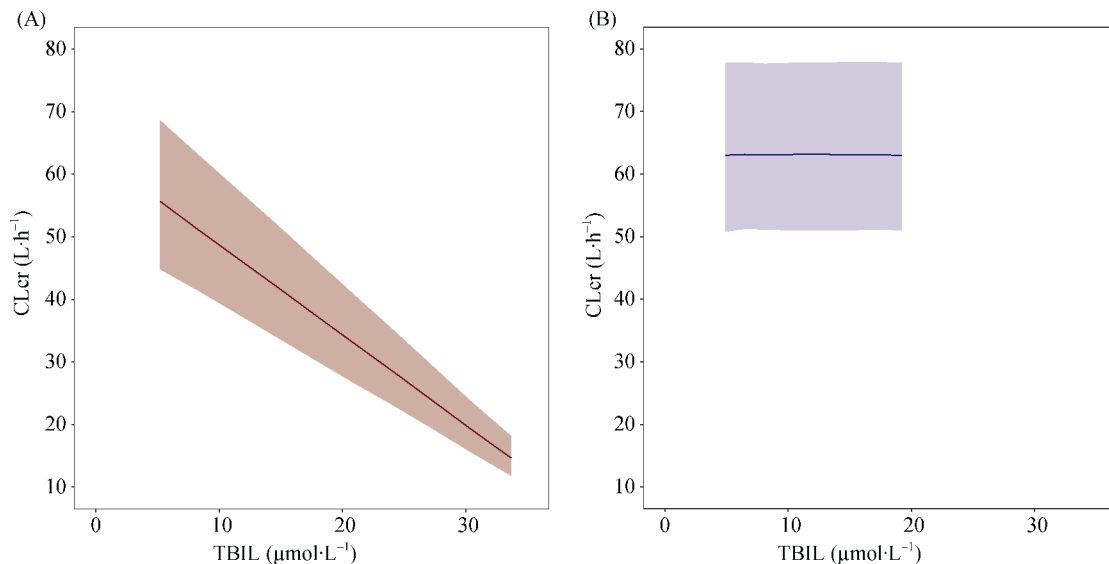


Fig. 1 A Monte Carlo simulation was carried out to describe the relationship between TBIL and CL in CHD patients (A) and healthy volunteers (B). The solid lines are the median of the clearance with related TBIL and the ribbon represent the simulation-based 90% confidence interval

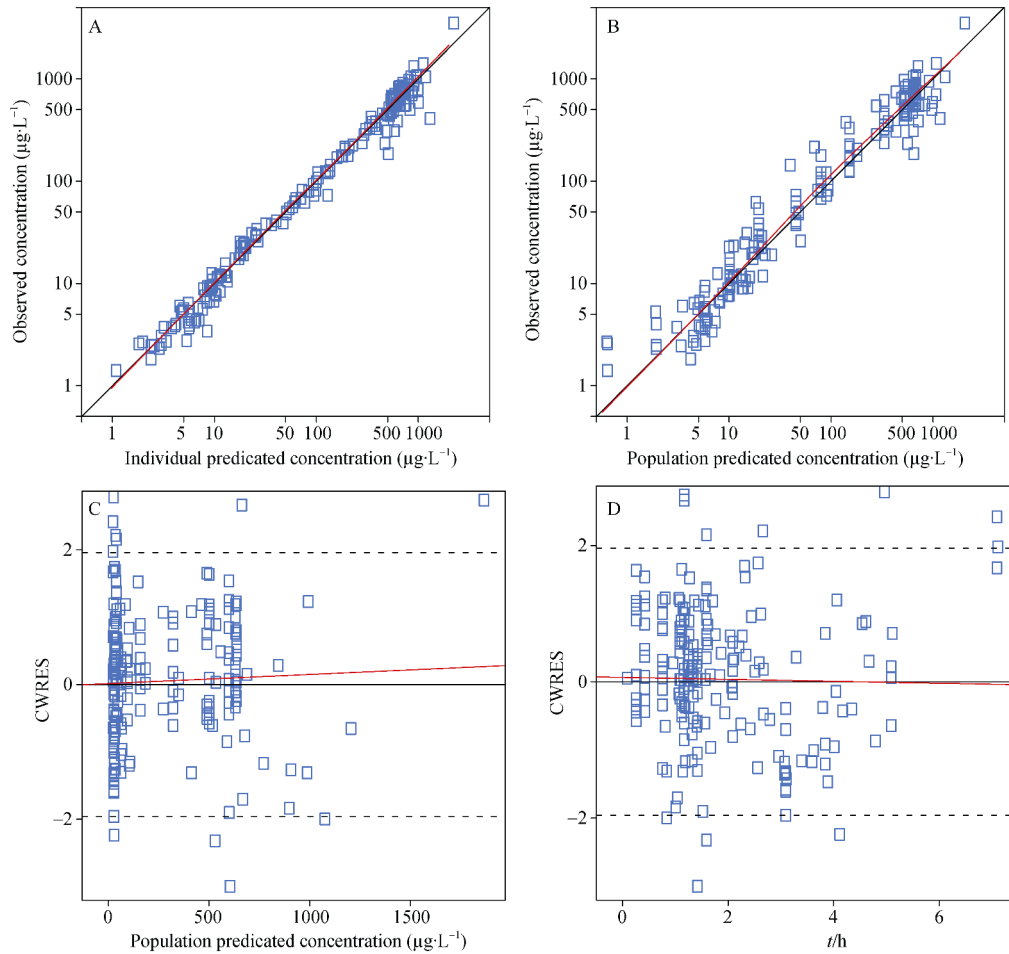


Fig. 2 Goodness-of-fit plots of the final model of STS: (A) observed vs individual-predicted concentrations; (B) observed vs population-predicted concentrations; (C) conditional weighted residuals vs population-predicted concentrations; (D) conditional weighted residuals vs time. The black lines in (A) and (B) are identity lines and that in (C) and (D) are zero lines. The red lines in (A) and (B) represent regression lines via locally weighted polynomial regression (LOESS) and that in (C) and (D) are linear regression lines

The results of the VPC plots confirmed the robustness of the final model (Fig. 3). The 10th, 50th, and 90th percentiles of the concentration-time curves were determined from 1000 Monte Carlo simulations. Most of ob-

served concentrations were contained within the 90th percentile simulation, indicating that the fit of the model was acceptable in terms of visual and statistical biases of the prediction.

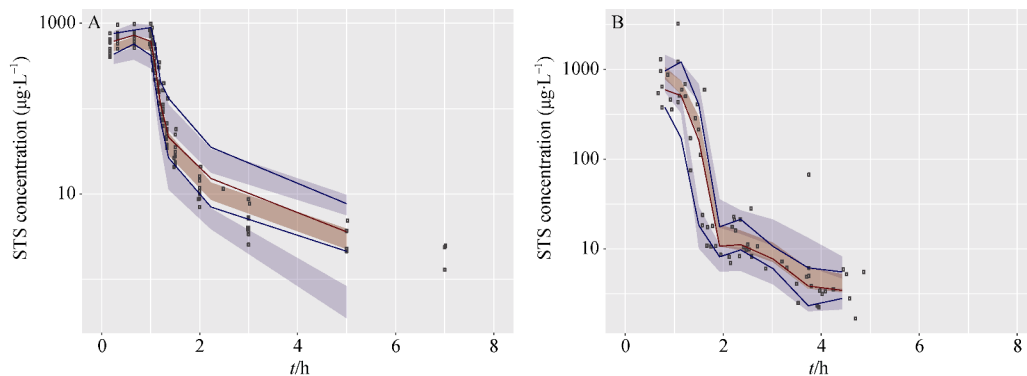


Fig. 3 Visual predictive check plots for the final model of STS in healthy volunteers (A) and CHD patients (B). The dots represent observed concentrations. The blue lines and the blue areas represent the 10th and 90th percentiles of predicted concentrations and their simulation-based 95 % confidence interval, respectively. The red line and the red area represent the 50th percentiles of predicted concentrations and its simulation-based 95 % confidence interval

Discussion

In this study, the PK of STS in the CHD patients was first compared with that in healthy volunteers using a PPK method, with results showing that the CL of STS differed between the two populations. Specifically, the CL of STS was lower in the CHD patients than in the healthy volunteers and was affected by TBIL.

The underlying mechanism of the lower CL of STS in the CHD patients is likely the relatively slow STS metabolism in the CHD patients. The predominant metabolic pathway for TSA in rats involves NQO1-mediated quinone reduction and subsequent glucuronidation [7]. This metabolic pathway has been confirmed with other tanshinones, including dihydro-tanshinone I and cryptotanshinone [18–19]. This evidence strongly suggests that the metabolic elimination of STS is mediated by NQO1, as STS is a sulfonated form of TSA with the same quinone molecular structure. During ischemia–reperfusion in CHD patients, myocardial oxygen radicals form quickly and accumulate to induce radical-induced injury [20]. NQO1 directly scavenges oxygen radicals in an NAD(P)H-dependent manner [21]. Therefore, we speculated that the overproduction of oxygen radicals in CHD patients competed with STS for NQO1 activity, resulting in relatively slow elimination of STS, whereas metabolism of STS was unaffected in healthy volunteers, because the absence of excessive oxygen radicals did not lead to diminished NQO1 activity. However, the mechanism of STS metabolism mediated by NQO1 in CHD patients remains to be elucidated.

As noted, the CL of STS in CHD patients was also affected by TBIL. A decrease in CL and high STS concentrations were observed in patients with higher TBIL levels. Serum bilirubin level reflects liver or biliary tract function [22–23], and STS is metabolized by the liver and excreted in the bile [3,9], suggesting that changes in hepatic or biliary tract function in CHD patients might influence STS metabolism and elimination. Therefore, it is physiologically plausible that the CL of STS will decrease as the TBIL level increases. Because of the limited sample size in this study, expanded investigations are necessary to confirm the effects of TBIL on STS elimination in CHD patients.

The final model suggested that the population values of CL in CHD patients were lower than those in healthy volunteers, decreasing from 88% to 23% when TBIL increased from 5.2 to 33.7 $\mu\text{mol}\cdot\text{L}^{-1}$. The final model also showed a linear relationship between TBIL and CL in CHD patients, where a one unit increase in TBIL resulted in a 2.28% decrease in CL while TBIL did not significantly affect the CL of STS in healthy subjects. This suggests that when patient TBIL increases from the median value (10 $\mu\text{mol}\cdot\text{L}^{-1}$) to the upper limit of the normal value (20.4 $\mu\text{mol}\cdot\text{L}^{-1}$), the STS CL decreases from 48.7 to 33.8 $\text{L}\cdot\text{h}^{-1}$, and the STS dosage should be

adjusted to approximately 75% of the original dose. A previous study reported that Danshen treatment increased the TBIL levels ($P < 0.05$) in CHD patients after 3 months of follow-up [24]. This result indicates that dosage adjustment of STS is necessary, because higher STS doses can increase TBIL levels, and higher TBIL can lower the STS CL further, resulting in STS accumulation. It should be noted that extrapolation of our final model equation should be performed with caution, because the TBIL range studied was limited.

The covariates of stable angina, unstable angina, non-ST-elevation myocardial infarction, and acute heart failure did not have significant, independent effects on the PK parameter of STS in CHD patients. Hospitalized CHD patients are generally diagnosed with unstable angina or non-ST-elevation myocardial infarction, which might be accompanied by acute heart failure [11]. Accordingly, stable angina, unstable angina, non-ST-elevation myocardial infarction, and acute heart failure represented the progression of CHD and were coded as covariates during PPK analysis. Previous studies examined the effect of heart failure on drug PK based on the hypothesis that reduced blood flow in the organs of elimination could lower CL, but the results were controversial. The CL of lidocaine was decreased in patients with heart failure, whereas that of ibutilide did not appear to be altered in these patients [12, 25]. These disease-progress-related factors could not predict STS PK independently in our study.

Additionally, we evaluated the influence of concomitant drugs on the PK of STS. Clopidogrel and STS are substrates of CYP3A4 and P-glycoprotein [8, 26], and most ARBs and STS are eliminated mainly via bile excretion [9, 27], which suggests possible effects of clopidogrel or ARBs on STS PK. However, clopidogrel and ARBs were not found to be significant during covariate screening, which agreed with the findings of a previous study that Danshen extract containing TSA did not alter the PK of clopidogrel [26]. These results indicate that the influence of common concomitant medications for CHD on STS PK might be limited. Further research is needed to confirm this due to the limited sample size of our study.

We did not find that demographic characteristics, including gender, age, and weight, affected STS CL. This is likely due to the relatively homogeneous patient population included in this study.

A limitation of the study is the relatively small sample size of CHD patients. Larger sample sizes that include more CHD patients with abnormal TBIL levels are needed for future studies. Large TBIL spans within a study cohort will facilitate determination of concrete relationship between CL and TBIL in CHD patients. Moreover, we did not include patients with chronic heart failure due to left ventricular dysfunction, because these patients had restricted sodium and water intake. It is possible that chronic heart failure is an in-

dependent predictor of the PK of STS in CHD patients. Further studies with larger sample sizes and dedicated study designs are required.

In conclusion, this represents the first PPK study of STS in CHD patients. The results showed that STS CL was lower in CHD patients than in healthy volunteers. Additionally, TBIL was identified as a significant covariate of STS PK in CHD patients. These results are clinically important for optimizing STS dosages in CHD patients. When patients present with abnormal TBIL, the STS CL should decrease significantly, and the STS dose should be adjusted according to TBIL level.

Acknowledgments

We thank GAO Yu-Cheng for technical help.

References

- [1] Wang BL, Wang H, Wang E, et al. Isolation and structure characterization of related impurities in Sodium Tanshinone IIA Sulfonate by LC/ESI-MSⁿ and NMR [J]. *J Pharmaceut Biomed*, 2012, **67-68**: 36-41.
- [2] Chen Y, Tu JH, He YJ, et al. Effect of sodium tanshinone II A sulfonate on the activity of CYP1A2 in healthy volunteers [J]. *Xenobiotica*, 2009, **39**(7): 508-513.
- [3] Mao SJ, Jin H, Bi YQ, et al. Ion-pair reversed-phase HPLC method for determination of sodium tanshinone IIA sulfonate in biological samples and its pharmacokinetics and biodistribution in mice [J]. *Chem Pharm Bull*, 2007, **55**(5): 753-756.
- [4] He TT, Zou QG, Feng ZB, et al. Study of sodium tanshinone II A sulfonate tissue distribution in rat by liquid chromatography/tandem mass spectrometry [J]. *Arzneimittel-Forsch*, 2010, **60**(11): 660-666.
- [5] Chen WZ, Dong YL, Wang CG, et al. Pharmacological studies of sodium tanshinone II-A sulfonate [J]. *Acta Pharm Sin*, 1979, **14**(5): 277-283.
- [6] Ouyang DS, Huang WH, Chen D, et al. Kinetics of cytochrome P450 enzymes for metabolism of sodium tanshinone IIA sulfonate *in vitro* [J]. *Chin Med*, 2016, **11**: 11.
- [7] Wang QO, Hao HP, Zhu XX, et al. Regioselective glucuronidation of tanshinone IIA after quinone reduction: identification of human UDP-glucuronosyltransferases, species differences, and interaction potential [J]. *Drug Metab Dispos*, 2010, **38**(7): 1132-1140.
- [8] Chen D, Lin XX, Huang WH, et al. Sodium tanshinone IIA sulfonate and its interactions with human CYP450s [J]. *Xenobiotica*, 2016, **46**(12): 1085-1092.
- [9] Sun JH, Yang M, Han J, et al. Profiling the metabolic difference of seven tanshinones using high-performance liquid chromatography/multi-stage mass spectrometry with data-dependent acquisition [J]. *Rapid Commun Mass Sp*, 2007, **21**(14): 2211-2226.
- [10] Qin WW, Wang B, Lu XP, et al. Determination of Sodium Tanshinone IIA Sulfonate in human plasma by LC-MS/MS and its application to a clinical pharmacokinetic study [J]. *J Pharmaceut Biomed*, 2016, **121**: 204-208.
- [11] Chinese Society of Cardiology. Guideline for diagnosis and treatment of patients with unstable angina and non-ST-segment elevation myocardial infarction [J]. *Chin J Cardiol*, 2007, **35**(04): 295-304.
- [12] Zito RA, Reid PR. Lidocaine kinetics predicted by indocyanine green clearance [J]. *New Engl J Med*, 1978, **298**(21): 1160-1163.
- [13] Smithburger PL, Kane-Gill SL, Seybert AL. Drug-drug interactions in cardiac and cardiothoracic intensive care units: an analysis of patients in an academic medical centre in the US [J]. *Drug Safety*, 2010, **33**(10): 879-888.
- [14] Cardiology Chinese Society. Guideline for diagnosis and treatment of patients with chronic stable angina [J]. *Chin J Cardiol*, 2007, **35**(03): 195-206.
- [15] Keizer RJ, van Benten M, Beijnen JH, et al. Pirana and PCluster: A modeling environment and cluster infrastructure for NONMEM [J]. *Comput Meth Prog Bio*, 2011, **101**(1): 72-79.
- [16] Lindbom L, Ribbing J, Jonsson EN. Perls-speaks-NONMEM (PsN)-a Perl module for NONMEM related programming [J]. *Comput Meth Prog Bio*, 2004, **75**(2): 85-94.
- [17] Jonsson EN, Karlsson MO. Xpose-an S-PLUS based population pharmacokinetic/pharmacodynamic model building aid for NONMEM [J]. *Comput Meth Prog Bio*, 1999, **58**(1): 51-64.
- [18] Dai HX, Wang MM, Li XR, et al. Structural elucidation of *in vitro* and *in vivo* metabolites of cryptotanshinone by HPLC-DAD-ESI-MSⁿ [J]. *J Pharmaceut Biomed*, 2008, **48**(3): 885-896.
- [19] Liu J, Wu JL, Wang XR, et al. Study of the phase I and phase II metabolism of a mixture containing multiple tanshinones using liquid chromatography/tandem mass spectrometry [J]. *Rapid Commun Mass Sp*, 2007, **21**(18): 2992-2998.
- [20] Hamilton KL. Antioxidants and cardioprotection [J]. *Med Sci Sports Exerc*, 2007, **39**(9): 1544-1553.
- [21] Zhu H, Li YB. NAD(P)H: Quinone oxidoreductase 1 and its potential protective role in cardiovascular diseases and related conditions [J]. *Cardiovasc Toxicol*, 2012, **12**(1): 39-45.
- [22] Emoto-Yamamoto Y, Iida S, Kawanishi T, et al. Population pharmacokinetics of erlotinib in Japanese patients with advanced non-small cell lung cancer [J]. *J Clin Pharm Ther*, 2015, **40**(2): 232-239.
- [23] Lee JY, Hahn HJ, Son IJ, et al. Factors affecting the apparent clearance of tacrolimus in Korean adult liver transplant recipients [J]. *Pharmacotherapy*, 2006, **26**(8): 1069-1077.
- [24] Liu BY, Du YH, Cong LX, et al. Danshen (*Salvia miltiorrhiza*) compounds improve the biochemical indices of the patients with coronary heart disease [J]. *Evid-Based Compl Alt*, 2016, **2016**: 9781715.
- [25] Tisdale JE, Overholser BR, Sowinski KM, et al. Pharmacokinetics of ibutilide in patients with heart failure due to left ventricular systolic dysfunction [J]. *Pharmacotherapy*, 2008, **28**(12):

1461-1470.

- [26] Lee JH, Shin YJ, Kim HJ, *et al.* Danshen extract does not alter pharmacokinetics of docetaxel and clopidogrel, reflecting its negligible potential in P-glycoprotein- and cytochrome P4503A-mediated herb-drug interactions [J]. *Int J Pharmaceut*,

2011, **410**(1-2): 68-74.

- [27] Michel MC, Foster C, Brunner HR, *et al.* A systematic comparison of the properties of clinically used angiotensin II type 1 receptor antagonists [J]. *Pharmacol Rev*, 2013, **65**(2): 809-848.

Cite this article as: QIN Wei-Wei, WANG Li, JIAO Zheng, WANG Bin, WANG Cheng-Yu, QIAN Li-Xuan, QI Wei-Lin, ZHONG Ming-Kang. Lower clearance of sodium tanshinone IIA sulfonate in coronary heart disease patients and the effect of total bilirubin: a population pharmacokinetics analysis [J]. *Chin J Nat Med*, 2019, **17**(3): 218-226.